PAPER • OPEN ACCESS

A novel detector system for KATRIN to search for keV-scale sterile neutrinos

View the article online for updates and enhancements.

AAS | **IOP** Astronomy ebooks

Part of your publishing universe and your first choice for astronomy, astrophysics, solar physics and planetary science ebooks.

iopscience.org/books/aas

A novel detector system for KATRIN to search for keV-scale sterile neutrinos

Susanne Mertens[1,2,11] ⓘ**, Antonio Alborini**[3]**,
Konrad Altenmüller**[3]**, Tobias Bode**[1]**, Luca Bombelli**[3]**,
Tim Brunst**[1,2]**, Marco Carminati**[5]**, David Fink**[1]**, Carlo Fiorini**[5]**,
Thibaut Houdy**[1,2]**, Anton Huber**[4]**, Marc Korzeczek**[4]**,
Thierry Lasserre**[2,6,7,8]**, Peter Lechner**[9]**, Michele Manotti**[3]**,
Ivan Peric**[4]**, David C Radford**[10]**, Daniel Siegmann**[1,2]**,
Martin Slezák**[1]**, Kathrin Valerius**[4]**, Joachim Wolf**[4] **and
Sascha Wüstling**[4]

[1] Max Planck Institute for Physics, Föhringer Ring 6, D-80805 München, Germany
[2] Technische Universität München, Arcisstraße 21, D-80333 München, Germany
[3] XGLab SRL, Bruker Nano Analytics, Via Conte Rosso 23, Milano, Italy
[4] Karlsruhe Institute of Technology, Hermann-von-Helmholtz-Platz 1, D-76344 Eggenstein-Leopoldshafen, Germany
[5] Politecnico di Milano, Dipartimento di Elettronica, Informazione e Bioingegneria, Piazza Leonardo da Vinci, 32, I-20133 Milano, Italy
[6] Commissariat à l'énergie atomique et aux énergies alternatives, Centre de Saclay, DRF/IRFU, F-91191 Gif-sur-Yvette, France
[7] Institute for Advanced Study, Technische Universität München, James-Franck-Str. 1, D-85748 Garching, Germany
[8] Astroparticule et Cosmologie, Université Paris Diderot, CNRS/IN2P3, CEA/IRFU, Observatoire de Paris, Sorbonne Paris Cité, F-75205 Paris Cedex 13, France
[9] Halbleiterlabor der Max Planck Gesellschaft, Otto-Hahn-Ring 6, D-81739 München, Germany
[10] Oak Ridge National Laboratory, 1 Bethel Valley Road, Oak Ridge, 37831 TN, United States of America

E-mail: mertens@mpp.mpg.de

CrossMark

Abstract

Sterile neutrinos appear in minimal extensions of the Standard Model of particle physics. If their mass is in the keV regime, they are viable dark matter

[11] Author to whom correspondence may be addressed.

candidates. One way to search for sterile neutrinos in a laboratory-based experiment is via the analysis of β-decay spectra, where the new neutrino mass eigenstate would manifest itself as a kink-like distortion of the β-decay spectrum. The objective of the TRISTAN project is to extend the KATRIN setup with a new multi-pixel silicon drift detector system to search for a keV-scale sterile neutrino signal. In this paper we describe the requirements of such a new detector, and present first characterization measurement results obtained with a 7 pixel prototype system.

(Some figures may appear in colour only in the online journal)

1. Introduction

Several theories beyond the Standard Model (SM) predict the existence of new types of neutrinos, so-called sterile neutrinos, which owe their name to the fact that they would not take part in any SM interaction. Right-handed partners for the known purely left-handed neutrinos are an example of such sterile neutrinos. While being a minimal extension of the SM, sterile neutrinos can tackle a large number of open questions. Very heavy, typically $\mathcal{O}(10^{14}\,\text{GeV})$, sterile neutrinos provide a natural explanation for the light mass of the active neutrinos via the seesaw mechanism [1] and could shed light on the matter–antimatter asymmetry of the universe via leptogenesis [2]. eV-scale sterile neutrinos can solve a number of anomalies found in short-baseline oscillation experiments, such as the well-known reactor anomaly [3]. The focus of this paper is on sterile neutrinos in the keV range, which are viable candidates for dark matter [4–6]. One notable feature of this candidate is that it can act as effectively cold or warm dark matter depending on its production mechanism in the early universe [7, 8].

The strongest experimental bounds on the existence of keV-scale sterile neutrino dark matter are currently obtained from astrophysical observations with telescopes, that search for a mono-energetic x-ray line arising from the decay of relic sterile neutrinos. These measurements limit the active-to-sterile mixing amplitude indicated as $\sin^2\Theta$ (which determines their interaction strength) to $\sin^2\Theta < 10^{-6} - 10^{-10}$ in a mass range of 1–50 keV [9, 10]. Furthermore, cosmological considerations and observations of structure formation can indirectly limit the allowed parameter space for sterile neutrino dark matter; for a detailed review see [11, 12]. Current laboratory-based limits are orders of magnitudes weaker than astrophysical bounds [11, 12].

A promising way to perform a laboratory-based sterile neutrino search is via β-decay [13–16]. In a β-decay an electron-flavor neutrino is emitted along with the β-electron. The corresponding continuous β-decay spectrum is a superposition of spectra corresponding to the different neutrino mass states m_i that comprise the electron neutrino flavor eigenstate. Due to the tiny mass differences of the three light neutrino mass eigenstates, this superposition cannot be resolved with current experiments such as the Karlsruhe Tritium Neutrino (KATRIN) experiment [17, 18]. However, sterile neutrinos with a mass m_s[12] significantly heavier than the mass of the known neutrino mass eigenstates m_{1-3}, would lead to a distinct distortion of the β-decay spectrum. The total differential tritium β-decay spectrum

---

[12] As sterile neutrinos are singlets under all SM gauge transformations, they can possess a Majorana mass of arbitrary scale. Throughout this paper we refer to sterile neutrinos as neutrino mass eigenstates, which, strictly speaking, are not purely sterile, but can have an admixture of the active neutrino flavors.
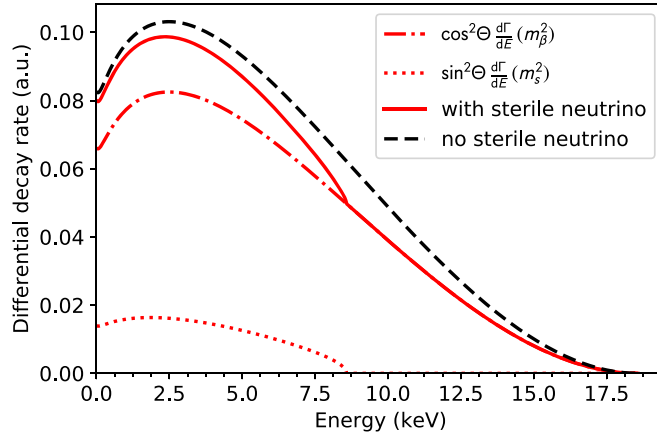
Figure 1. Imprint of a heavy, mostly sterile, neutrino with a mass of $m_s = 10$ keV and an unphysical large mixing angle of $\sin^2\Theta = 0.2$ on the tritium β-decay spectrum. The red dotted line depicts the decay branch into a sterile neutrino, the red dashed-dotted line shows the regular decay branch into a light active neutrino. The solid red line is the resulting superposition of the two spectra, which includes a kink-like distortion. As a comparison, the black dashed line shows a spectrum without a sterile neutrino.

$$\frac{\mathrm{d}\Gamma}{\mathrm{d}E} = \cos^2\Theta \, \frac{\mathrm{d}\Gamma}{\mathrm{d}E}(m_\beta^2) + \sin^2\Theta \, \frac{\mathrm{d}\Gamma}{\mathrm{d}E}(m_s^2) \tag{1}$$

would be a superposition of the standard spectrum, with the endpoint governed by the effective electron neutrino mass m_β, and a spectrum with a significantly reduced endpoint corresponding to the decay into a sterile neutrino of mass m_s. The amplitude of the additional decay branch would be governed by the active-sterile mixing amplitude $\sin^2\Theta$. Hence, sterile neutrinos would manifest themselves as a local kink-like feature and a broad spectral distortion below $E_{\mathrm{kink}} = E_0 - m_s$, see figure 1.

With an endpoint of $E_0 = 18.6$ keV the super-allowed β-decay of tritium is well suited for a keV-scale sterile neutrino search. Due to the short half life of 12.3 years, high decay rates can be achieved with reasonable amounts of tritium. Furthermore, a kink-like sterile neutrino signature would be a distinct feature in the otherwise fully smooth tritium β-decay spectrum [15].

2. The TRISTAN project

The idea of the TRISTAN project is to utilize the unprecedented tritium source luminosity of the KATRIN experiment for a high-precision keV-scale sterile neutrino search, by extending the experimental setup with a novel detector and read-out system.[13]

KATRIN's prime goal is a direct probe of the absolute neutrino mass scale via a precise measurement of the tritium beta decay spectrum close to its endpoint, where the imprint of the neutrino mass is maximal. For this purpose, KATRIN combines a high-activity (10^{11} decays per second) gaseous molecular tritium source with a high-resolution ($\Delta E \sim 1$ eV) spectrometer. The β-electrons are guided along magnetic field lines from the so-called windowless

---

[13] The KATRIN experiment has the potential to search for light sterile neutrinos without any hardware modification [20–22]. In contrast to keV-scale sterile neutrinos, the signal of an eV-scale sterile neutrino could be rather large (1%), would however appear close to the endpoint, where the signal rate is low.
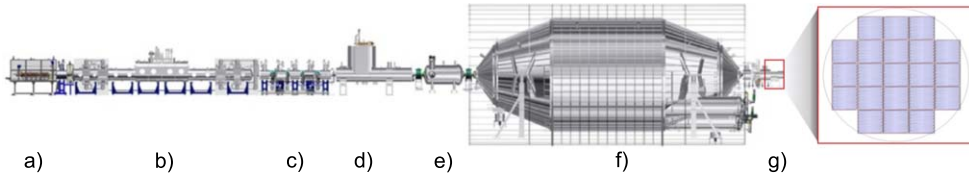
Figure 2. The left-hand side of the figure depicts the KATRIN apparatus: (a) rear section, (b) windowless gaseous tritium source (WGTS), (c) differential pumping section, (d) cryogenic pumping section, (e) pre-spectrometer, (f) main spectrometer, (g) detector section. For a detailed overview of KATRIN see [17]. For the TRISTAN project the 148 pixel Si-PIN focal plane detector [19] would be replaced by a $\approx$3500 pixel silicon drift detector system, displayed enlarged on the right-hand side of the figure. The baseline design comprises 21 so-called detector modules, each with 166 pixels and a side length of 4 cm. Each pixel has a hexagonal shape and a diameter of 3 mm. The total detector diameter is about 20 cm.

gaseous tritium source to the spectrometer. The latter is operated as a magnetic adiabatic collimation and electrostatic filter [23, 24], which transmits electrons with kinetic energies larger than the spectrometer's retarding potential. By observing the number of transmitted electrons for different filter voltages U in a range of about $E_0 - 60$ eV $< qU < E_0 + 5$ eV (where q is the electron charge) the integral tritium β-decay spectrum is obtained. The rate of electrons is detected with a 148 pixel focal plane detector [19, 25] situated at the exit of the KATRIN spectrometer. The detector system is equipped with a post-acceleration electrode (PAE), that increases the kinetic energy of all electrons by a fixed amount of up to 20 keV [19]. Figure 2 gives an overview of the experimental setup.

Operating KATRIN to search for keV-scale sterile neutrinos requires extending the measurement interval to cover the entire tritium β-decay spectrum, i.e. to set the filter voltage to values much lower than in standard operation [15]. In this new mode of operation the number of transmitted electrons will be a few orders of magnitudes higher than in normal KATRIN operation mode. The current silicon focal plane detector is not designed to handle such high count rates. Accordingly, the main objective of the TRISTAN project is to develop a new detector and read-out system, capable of revealing very small spectrum distortions, and handling rates of up to 10^8 counts per second (cps).

The main challenge of a keV-scale sterile neutrino search is the precise understanding of the entire spectrum on the parts-per-million (ppm) level, in order to be able to start probing sterile-active mixing angles of cosmological interest. In order to reduce systematic uncertainties and avoid false-positive signals, a combination of an integral and a differential measurement mode is planned: the integral mode makes use of the high-resolution spectrometer and a counting detector (analogous to the normal KATRIN measurement mode). This mode requires an extremely stable counting rate. In the differential mode, the spectrometer is operated at low filter voltage continuously and the detector itself determines the energy of each electron. This mode requires an excellent energy resolution and a precise understanding of the detector response even at high counting rates. The two measurement modes are prone to different systematic uncertainties and hence allow to cross check each other.

In both the integral and differential measurement mode, an increased magnetic field to about 12 G in the analyzing plane is necessary to assure adiabatic transport of high-surplus-energy electrons through the main spectrometer [26]. This is technically feasible by increasing the electric current of the large KATRIN air-coil system [27, 28].
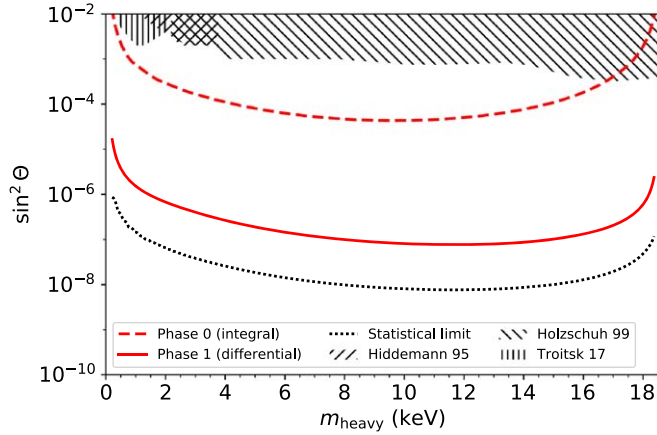
Figure 3. This figure shows the 95% C L statistical sensitivity for different stages of TRISTAN. Phase-0 (dashed red line): Integral measurement with a total statistics of 6×10^{11} electrons. This could be achieved with a 7 d measurement campaign at a reduced signal rate of 10^6 cps. The rate reduction can be obtained by reducing the amount of tritium and/or the acceptance angle. This scenario could in principle still be realized with the current KATRIN detector and read-out system. Phase-1 (solid red line): Differential measurement with a total statistics of 10^{16} electrons. For this scenario we assume a 3 years measurement period and a signal rate of 10^8 cps. This signal rate is obtained with a 100-fold reduced tritium column density (with respect to nominal KATRIN operation), for which systematic effects related to scattering of electrons with gas molecules and pile-up effects are significantly reduced. We assume a constant energy resolution of 300 eV FWHM. 3) Differential measurement with total statistics of 10^{18} electrons. This is the statistical limit that could be reached after a 3 years data-taking phase with the full source strength of the KATRIN experiment. The grey dashed area depicts the current laboratory-based limits [29–31].

TRISTAN is currently an R&D effort for an experiment to take place after the completion of the neutrino mass measurement of KATRIN, prospectively in 2025. The design goal of TRISTAN is to achieve a sensitivity of $\sin^2\Theta < 10^{-6}$. Figure 3 displays the targeted TRISTAN sensitivity.

3. Requirements on the detector system

The final TRISTAN detector is designed with the goal of at least achieving a sensitivity to active-sterile mixing angles in the < ppm-level, see figure 3. Correspondingly, the systematic uncertainties have to be on the same order of magnitude. From a purely statistical point of view, a ppm sensitivity can be reached with a total statistics of 10^{16} electrons. Assuming a data taking period of 3 years, this leads to a count rate of $n_{tot} = 10^8$ cps on the entire detector. To minimize the pile-up probability a count rate per pixel of maximally 10^5 cps is foreseen. This leads to a minimum of 1000 pixels. The maximum number of pixels is limited to keep the complexity and cost at a manageable level. This is especially true as a sophisticated front-and back-end read-out electronics will be needed to ensure low noise, good energy resolution, high linearity, and the ability to tag charge-sharing, and backscattering of electrons from the detector surface.

In order to maximize statistics and avoid unused pixels, the detector size should be close to the size of the electron beam. The magnetic flux $\Phi = B \cdot A$, where B is the magnetic field

and A is the beam area, is conserved along the entire KATRIN beamline. Hence, the electron beam area at the detector position is determined by the corresponding magnetic field B_{det}. B_{det} can easily by varied between 0.5 and 4.5 T by changing the electric current in the magnet and by varying the position of the detector with respect to the detector magnet, which in turn allows for variable detector diameters.

The optimization of the pixel and detector size is driven by the aim of minimizing both charge-sharing between neighboring detector pixels and backscattering of electrons from the detector surface.

Minimal charge-sharing is obtained by choosing the largest pixel area that does not compromise the energy resolution and the charge collection time of the detector. The backscattering effect impacts the choice of pixel and detector size in multiple ways:

- To minimize the backscattering probability the pitch angle (angle between the electron's momentum vector and magnetic field vector) at the detector should be $\theta_{det} < 20°$. The maximal pitch angle is determined by $\theta_{max} = \arcsin\left(\sqrt{\frac{B_{det}}{B_{max}}}\right)$, and hence can be reduced by placing the detector in a magnetic field B_{det} smaller than the maximal magnetic field in the system $B_{max} = 6~T$. The pitch angle is further reduced by applying a post-acceleration voltage V_{PAE}. For $V_{PAE} = 20~kV$, the desired pitch angle can be obtained with a detector magnetic field of $B_{det} \lesssim 1.5~T$. Correspondingly a minimal detector radius or $r_{det} \gtrsim 6$ cm is needed.
- By choosing $B_{det} < B_{max}$, backscattered electrons can be magnetically backreflected onto the detector surface. By increasing the back-reflection probability the number of lost electrons can be reduced. The back-reflection probability increases with the ratio $\frac{B_{max}}{B_{det}}$. This again supports the choice of a small detector magnetic field and consequently a large detector area.
- Finally, it is preferred that the magnetically backreflected electrons hit the same or at most a neighboring pixel. In this case it would be possible to identify these events by applying a cut based on interarrival time for these spatially close events. The spatial distance of subsequent detector hits is mainly governed by the cyclotron radius of the electrons, which decreases with the magnetic field as $r_{cycl} \propto \frac{1}{B}$. Consequently, to maximize the probability that a backreflected electron returns to the same or at most a neighboring pixel, the detector should be placed in a relatively large magnetic field, which would support the choice of a small detector area of $r_{det} \lesssim 11$ cm.

A detailed optimization based on Monte-Carlo simulations was performed taking into account all above-mentioned effects [32]. For this purpose the simulation software KASSIO-PEIA [33], developed by the KATRIN collaboration, was used. It allows to compute the trajectory of electrons in the electromagnetic field setup of the KATRIN experiment. Moreover, it includes a module, called KESS [34], which simulates precisely the interactions of keV-scale electrons in silicon.

In the simulation $\mathcal{O}(10^6)$ electrons with energies up to 18 keV were started isotropically in the maximal magnetic field, and were tracked towards the detector, inside which interactions with silicon were simulated. Backscattered (primary and secondary) electrons are again tracked in the electromagnetic fields of the KATRIN vacuum system, where some of these electrons are reflected back to the detector by the maximum magnetic field. In this way, multiple backscatterings with the exact interarrival times and detector hit positions are taken into account. The simulations were performed for several detector positions, pixel sizes, and different post-acceleration voltages. Fixing the number of detector pixels to 3500 and the post-acceleration voltage to 20 keV, the optimal performance was found for a pixel diameter
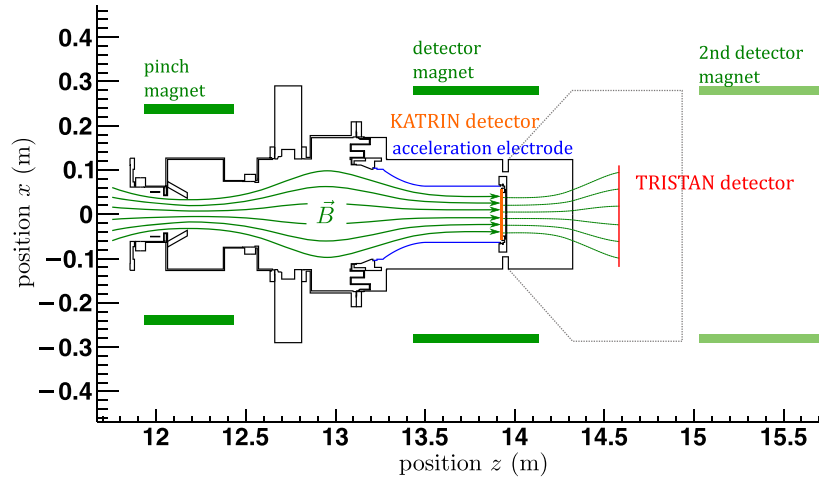
Figure 4. KASSIOPEIA simulation setup of the detector section of the KATRIN experiment. Electrons are guided by the magnetic field lines (green) onto the detector (red). The magnetic field is created by the pinch and detector magnet. An additional magnet can be placed behind the detector to make the field lines intersect perpendicularly with the detector surface. In blue the post-acceleration electrode (PAE) which can be set to up to 20 keV is displayed. In orange the current position of the KATRIN focal plane detector is shown and in red the position of the TRISTAN is indicated.

of 3 mm and a detector area of $A = \pi \cdot (10 \, \text{cm})^2$, corresponding to a detector magnetic field of 0.7 T. Figure 4 shows the simulated beamline section.

To observe the kink-like structure an energy resolution of approximately 300 eV at 30 keV is needed [16]. For this reason the silicon drift detector (SDD) technology is extremely suitable. It allows for very low noise levels even for large pixel diameters (3 mm) and high count rates (10^5 cps per pixel). First measurements with a 2 mm pixel diameter SDD prototype detector, described in section 5, demonstrate an excellent resolution of about 140 eV (FWHM) for 6 keV x-rays.

Unlike in the case of x-ray detection, the challenge of the detection of electrons is that they unavoidably deposit energy in the non-fully-active entrance window of the detector. Moreover, charge-sharing and backscattering can lead to very small energy depositions. In order to be able to identify these events not only an excellent energy resolution but also a low energy threshold of about 1 keV is of upmost importance. For these reasons, an extremely thin entrance window is needed. Assuming the simplified situation of a completely dead entrance volume, a thickness of < 50 nm is needed in order to meet the requirements with respect to energy threshold and resolution. This poses a new challenge for the production technique of SDDs [35].

A high performance read-out electronics is foreseen to assure high energy resolution and control of systematic effects. To optimize the noise performance of the system, SDDs with integrated nJFET are considered. In this case, the front-end ASIC only completes the feedback loop of the pre-amplification and can be placed at some distance from the detector anode. This is advantageous for a large-area detector, such as the TRISTAN detector array, where an installation of the pre-amplification close to the anode poses technical challenges.

A challenge of the back-end electronics is to minimize ADC nonlinearities. ADC nonlinearities can lead to discontinuous distortions of the differential β-decay spectrum, which

(a)   (b)
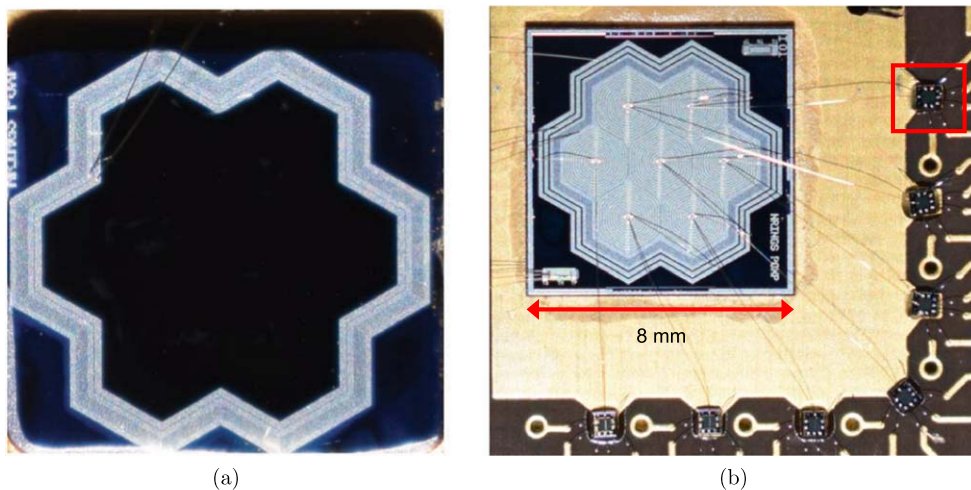
Figure 5. Close-up photographs of the detector chip. (a) The photograph shows the entrance window side of the detector which has no structuring of the individual cells. A common electrode for depletion voltage and guard-ring surrounds the detector. (b) Read-out side of detector chip. The drift rings are arranged around each individual cell anode and in this way define the cell shape and size. The anodes are bonded to individual CUBE preamplifier ASICs (one of them is circled in red square) which are arranged around the chip.

could possibly mimic the signature of sterile neutrinos and hence reduce the sensitivity of the experiment. A detailed study demonstrated that using a waveform digitizing ADC (as opposed to a peak-sensing ADC) helps to significantly average out the effect of nonlinearities [36]. Moreover, waveform digitization with high sampling frequency of about 100 MHz helps to efficiently detect pile-up events.

Finally, the field-programmable gate array (FPGA) of the back-end system has to provide the option of detecting not only pile-up events, but also multiplicities in neighboring or next-to-neighboring pixels. This option is needed to tag both charge-sharing and backscattering events. Fast processing and histogramming at the FPGA level is preferred for high-rate data taking phases in order to keep the data output at a manageable level. For characterization and validation, an event-by-event read-out mode will also be necessary.

4. Prototype silicon drift detector setup

A 7 pixel prototype SDD system was fabricated to test the general performance and to investigate the specific requirements mentioned above. Figures 5(a) and (b) show photographs of the radiation entrance and read-out side of the sensor chip.

As radiation sensor a custom made monolithic SDD array produced by the Semiconductor Laboratory of the Max Planck Society (HLL) [37] was chosen. These SDDs have a shallow pn-junction as thin radiation entrance window. It is obtained by a low-energy boron implantation through a scattering oxide layer. The charge-collection inefficiency of the entrance window region corresponds to an effective 'dead' layer thickness of the order of 10 nm, that has been evaluated by optical spectrometry, x-ray spectroscopy, and charged particles [35]. In the entrance window area the silicon surface is terminated by an oxide layer with a thickness of several nm.

Each of the seven pixels has an almost hexagonal shape and a characteristic small anode, 90 μm, for a low detector capacitance of approximately 110 fF. The pixels are arranged in a gapless fashion so that no dead area inside the array is present. Arrays with a cell diameter of 0.25, 0.5, 1 and 2 mm were produced with a wafer thickness of 450 μm. In this work we present results obtained with 1 and 2 mm pixel diameter and 10 and 20 drift rings, respectively.[14]

For the prototype system presented in this work, the SDD has no integrated nJFET. Correspondingly, an charge-sensitive preamplifier (CSA) application-specific integrated circuit (ASIC) was placed in close vicinity to the detector in order to minimize the input stray capacitance of the amplifier, which is a critical parameter in setting its noise performance. The CUBE ASIC produced by the XGLab company [38] was chosen, which achieves unprecedented noise performances, equivalent to SDD systems with integrated read-out [39].

The CUBE ASIC is directly wire bonded to the pixel anode, as shown in figure 5. The amplifier features a field effect transistor (FET) in complementary metal oxide semiconductor technology whose high transconductance compensates possible additional capacitances by the wire bonds. The extremely low capacitance of the detector and front-end read-out leads to a low voltage (series) noise. This in turn allows operating the system at very short ($\leqslant 1\ \mu$s) trapezoidal filter peaking times, and hence to achieve very good energy resolutions at high rates [39]. The CSA is a pulsed-reset amplifier which is favorable for high rates since tail pile-up does not occur. Excellent energy resolution close to the Fano limit has been reported for this preamplifier [38].

As back-end read-out the DANTE digital pulse processor (DPP), also produced by XGLab, was used. It is used to digitize the signal with a sampling frequency of 125 MS s^{-1} and a resolution of 16 bit. Furthermore, the DPP applies a trapezoidal filter with user-defined peaking and gap time for energy reconstruction.

5. First characterization measurements

The main objective of this first measurement phase was to test the general performance of the detector. In particular we focused on the energy resolution, linearity and electronic noise of the system.

The measurements were performed at the Max Planck Institute for Physics in a dedicated setup, composed of a vacuum-tight stainless steel vessel with a cooling system, that can stably cool the detector to its optimal operating temperature of $-30\ ^\circ$C. The setup features a special holder for a variety of radioactive calibration sources. All measurements presented here were performed with x-ray and gamma sources.

A suitable calibration source to test the performance of the system is ^{55}Fe, which features two close-by x-ray lines, the MnKα and MnKβ line at 5.9 keV and 6.5 keV, respectively. A typical ^{55}Fe spectrum recorded with a 2 mm pixel-diameter SDD array at $-30\ ^\circ$C is shown in figure 6. The main peaks can be well approximated by Gaussian functions and show an excellent energy resolution of 139 eV (FWHM) at the 5.9 keV x-ray line.

The peak shapes show a small low energy tail, which can be explained by incomplete charge collection close to the entrance window [40, 41]. This feature will be more pronounced for electrons, since, due to their shorter mean free path in silicon, they unavoidably deposit a fraction their energy in the non- or only partially-sensitive entrance volume. Detailed characterizations of the 7 pixel prototype SDD with electron sources are currently ongoing.

---

[14] The maximum pixel diameter of the prototype system is only 2 mm, even though a 3 mm pixel diameter is foreseen for the final system, since at the moment of the prototype production a slightly different design was foreseen.
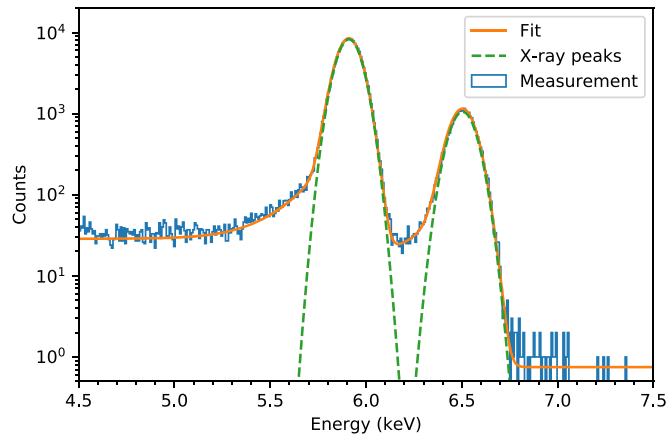
**Figure 6.** Energy spectrum of ^{55}Fe recorded with a 2 mm pixel diameter SDD array at −30° C. With an energy resolution of 139 eV (FWHM) @ 5.9 keV, the two lines are clearly separated. Two phenomenological functions similar to a hypermet (see [40], pp. 102) were used to fit the spectrum (orange). The Gaussian parts of the two peaks are indicated in green.
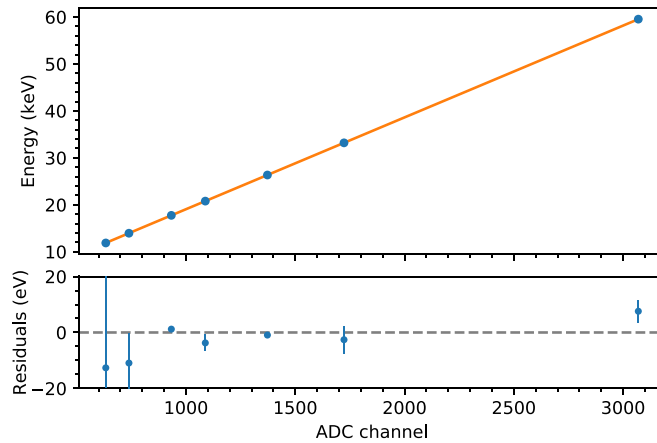
Figure 7. Linear calibration curve, based on an ^{241}Am spectrum. The blue dots correspond to the following photon lines: 11.9 keV (x-ray), 13.9 keV (x-ray), 17.8 keV (x-ray), 20.8 keV (x-ray), 26.3 keV (gamma), 33.2 keV (gamma), and 59.5 keV (gamma). The error bars contain the uncertainty of the line positions and the fit uncertainty. The maximal deviation from the linearity is 0.1% at the lowest energy peak of 11.9 keV.

To test the linearity of the system an ^{241}Am calibration source was used. It emits photons in a wide energy from from 10–60 keV, which is precisely the energy region of interest for TRISTAN. The maximum energy reached in the experiment would be the tritium endpoint at 18.6 keV, shifted by the post-acceleration voltage of up to 30 keV.

The result, displayed in figure 7, shows an excellent linearity over the entire energy range. All measured line positions deviate from linearity by < 0.1%. For the final TRISTAN experiment any energy scale distortions, which cannot be corrected for with a smooth calibration function, e.g. ADC nonlinearities, will play a major role, as discussed in [36].
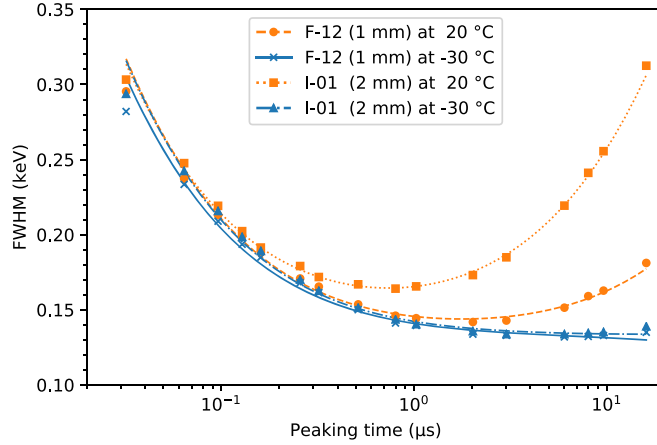
Figure 8. Energy resolution of the 5.9 keV of ^{55}Fe as a function of peaking time. The performance of the 1 and 2 mm pixel-diameter detector at room temperature (orange) and −30 °C (blue) is compared. At room temperature the noise (especially of the larger detector) is increased for large peaking times due to leakage current. For cooled detectors the leakage current is reduced to a negligible level, such that the performance of both pixel dimensions is equivalent.

Accordingly, detailed investigation concerning the choice of the most suitable DAQ system are currently ongoing.

To investigate the noise performance of the detector system, the energy resolution of the 5.9 keV MnKα line of ^{55}Fe was measured as a function of the peaking time. The peaking time is a parameter of the trapezoidal filter, applied to deduce the amplitude and hence the energy of an event from the waveform. It represents the time span over which the waveform is averaged, and hence reflects which noise components are dominant in the signal.

Figure 8 shows the typical dependence of the resolution on the peaking time for the 1 mm and 2 mm pixel diameter detector at room temperature and at −30 °C. The increase of noise at large peaking times at room temperature is due to leakage current. As expected, it is more pronounced for the 2 mm detector as the leakage current grows with the area of the pixel. At −30 °C, the leakage current is suppressed to a negligible level for both the 1 and 2 mm pixel diameter detector. This demonstrates that the performance is not degraded for larger pixel areas. This is an important requirement for the TRISTAN detector, which will use a 3 mm pixel diameter.

Due to the lower leakage current and also reduced 1/f noise (peaking-time-independent noise component), at −30 °C, an energy resolution of ⩽140 eV FWHM (corresponding to a minimal equivalent noise charge (ENC) of ⩽10 e_{rms}) can be reached for peaking times of about 1 μs. It is important to note that even for peaking times of less than 1 μs the energy resolution is still well below 300 eV (ENC < 20 e_{rms}). As TRISTAN will operate at high rates of up to 10^5 cps/pixel, a good energy resolution at short peaking times is essential.

6. Conclusion and outlook

A relevant search for a keV-mass sterile neutrino can be conducted with the KATRIN experiment, providing that the current focal plane detector is replaced with a new multi-pixel, high performance detector array, capable of coping with the high electron rates.

Detailed simulations show that the stringent requirements of such an experiment can be met by a several-thousand-pixel SDD system. The SDD design provides a suitable energy resolution for large pixel areas and high rates. As a special request of the TRISTAN project, new techniques are being explored to minimize the entrance window thickness.

A first seven-pixel prototype SDD array has been designed and was produced by the Semiconductor Laboratory of the Max Planck Society (HLL). First characterization measurements with the device verified the excellent performance of the complete detector array. Calibration measurements with x-ray lines of ^{55}Fe and ^{241}Am demonstrate an energy resolution of < 139 eV (FWHM) at 5.9 keV for peaking time of ≈ 1 μs, which is a key requirement for the high-rate application in TRISTAN. Further calibration measurements with x-ray and gamma-lines of ^{55}Fe and ^{241}Am show an excellent energy linearity of $< 0.1\%$ over an energy range of up to 10–60 keV.

Currently, the seven-pixel prototype SDD array is being characterized with dedicated electron calibration sources. In mid-2019, the production of the next-generation multi-pixel SDD sensor array by HLL will be completed, which will depict 1 of the 21 final TRISTAN detector modules. The final system will protectively be installed in the KATRIN beamline in 2025.

Acknowledgments

ORCID iDs

Susanne Mertens ⓘ https://orcid.org/0000-0002-7280-0854

References

[1] Mohapatra R N and Senjanović G 1980 *Phys. Rev. Lett.* **44** 912–5
[2] Canetti L and Shaposhnikov M 2010 *J. Cosmol. Astropart. Phys.* **2010** 001
[3] Abazajian K N *et al* 2012 Light sterile neutrinos: a white paper arXiv:1204.5379
[4] Dodelson S and Widrow L M 1994 *Phys. Rev. Lett.* **72** 17–20
[5] Shi X and Fuller G M 1999 *Phys. Rev. Lett.* **82** 2832–5
[6] Canetti L, Drewes M and Shaposhnikov M 2013 *Phys. Rev. Lett.* **110** 061801
[7] Zhu Q, Marinacci F, Maji M *et al* 2016 *Mon. Notices Royal Astron. Soc.* **458** 1159–80
[8] Murgia R, Merle A, Viel M, Totzauer M and Schneider A 2017 *J. Cosmol. Astropart. Phys.* **2017** 046
[9] Watson C R, Li Z and Polley N K 2012 *J. Cosmol. Astropart. Phys.* **2012** 018
[10] Boyarsky A, Iakubovskyi D, Ruchayskiy O and Savchenko V 2008 *Mon. Not. R. Astron. Soc.* **387** 1361–73
[11] Adhikari R *et al* 2017 *J. Cosmol. Astropart. Phys.* **2017** 025
[12] Boyarsky A, Drewes M, Lasserre T, Mertens S and Ruchayskiy O 2019 *Prog. Part. Nucl. Phys.* **104** 1–45
[13] Shrock R 1980 *Phys. Lett.* B **96** 159–64
[14] de Vega H, Moreno O, de Guerra E M, Medrano M R and Sánchez N 2013 *Nucl. Phys.* B **866** 177–95

[15] Mertens S, Lasserre T, Groh S *et al* 2015 *J. Cosmol. Astropart. Phys.* **2015** 020
[16] Mertens S, Dolde K, Korzeczek M *et al* 2015 *Phys. Rev.* D **91** 042005
[17] Angrik J *et al* (KATRIN Collaboration) 2005 https://publikationen.bibliothek.kit.edu/270060419/3814644
[18] Drexlin G, Hannen V, Mertens S and Weinheimer C 2013 *Adv. High Energy Phys.* **2013** 36
[19] Amsbaugh J *et al* 2015 *Nucl. Instrum. Methods Phys. Res.* A **778** 40–60
[20] Formaggio J A and Barrett J 2011 *Phys. Lett.* B **706** 68–71
[21] Riis A S and Hannestad S 2011 *J. Cosmol. Astropart. Phys.* **1102** 011
[22] Esmaili A and Peres O L G 2012 *Phys. Rev.* D **85** 117301
[23] Kruit P and Read F H 1983 *J. Phys. E: Sci. Instrum.* **16** 313
[24] Picard A *et al* 1992 *Nucl. Instrum. Methods Phys. Res.* B **63** 345–58
[25] Wall B *et al* 2014 *Nucl. Instr. Meth. Phys. Res.* A **744** 73–9
[26] Huber A 2015 Search for keV-Scale Sterile Neutrinos with KATRIN *Master's Thesis* Karlsruhe Institute of Technology
[27] Glück F, Drexlin G, Leiber B, Mertens S, Osipowicz A, Reich J and Wandkowsky N 2013 *New J. Phys.* **15** 083025
[28] Erhard M *et al* 2018 *J. Instrum.* **13** P02003
[29] Abdurashitov J N *et al* 2017 *JETP Lett.* **105** 753–7
[30] Holzschuh E, Kundig W, Palermo L, Stussi H and Wenk P 1999 *Phys. Lett.* B **451** 247–55
[31] Hiddemann K H, Daniel H and Schwentker O 1995 *J. Phys. G: Nucl. Part. Phys.* **21** 639
[32] Korzeczek M 2016 eV- and keV-sterile neutrino studies with KATRIN *Master's Thesis* Karlsruhe Institute of Technology
[33] Furse D *et al* 2017 *New J. Phys.* **19** 053012
[34] Renschler P 2011 KESS—A new Monte Carlo simulation code for low-energy electron interactions in silicon detectors *PhD thesis* Karlsruhe Institute of Technology
[35] Hartmann R, Strüder L, Kemmer J, Lechner P, Fries O, Lorenz E and Mirzoyan R 1997 *Nucl. Instrum. Methods Phys. Res.* A **387** 250–4
[36] Dolde K, Mertens S, Radford D, Bode T, Huber A, Korzeczek M, Lasserre T and Slezak M 2017 *Nucl. Instrum. Methods Phys. Res.* A **848** 127–36
[37] Lechner P *et al* 2001 *Proc. 11th Inbt. Workshop on Room Temperature Semiconductor X- and Gamma-Ray Detectors and Associated Electronics; Nucl. Instrum. Methods Phys. Res.* A **458** 281–7
[38] Bombelli L, Fiorini C, Frizzi T, Alberti R and Longoni A 2011 Cube, a low-noise CMOS preamplifier as alternative to JFET front-end for high-count rate spectroscopy *2011 IEEE Nuclear Science Symp. Conf. Record* pp 1972–5
[39] Bombelli L, Fiorini C, Frizzi T, Alberti R and Quaglia R 2012 High rate x-ray spectroscopy with cube preamplifier coupled with silicon drift detector *2012 IEEE Nuclear Science Symp. and Medical Imaging Conf. Record (NSS/MIC)* pp 418–20
[40] Eggert T 2004 Die spektrale Antwort von Silizium-Röntgendetektoren *Dissertation Technische Universität München* München
[41] Hartmann R, Hauff D, Lechner P, Richter R, Strüder L, Kemmer J, Krisch S, Scholze F and Ulm G 1996 *Proc. Seventh European Symp. on Semiconductor; Nucl. Instrum. Methods Phys. Res.* A **377** 191–6